

**Distinct photophysical properties in atom-precise silver and copper
nanocluster analogues**

Yan-Ling Li, Zhao-Yang Wang, Xiao-Hong Ma, Peng Luo, Chen-Xia Du* and Shuang-
Quan Zang*

*College of Chemistry and Molecular Engineering, Zhengzhou University, Zhengzhou
450001, China.*

*E-mail: zangsqzg@zzu.edu.cn; dcx@zzu.edu.cn

Materials and Methods

Materials and reagents

1,2-Dithiol-*o*-carborane was prepared by a literature method.^[S1] All other reagents and solvents were commercially available and used without additional purification.

Characterization.

Thermogravimetric (TG) analyses were performed on an SDT 2960 thermal analyzer from room temperature to 800 °C at a heating rate of 5 °C/min under a nitrogen atmosphere. To compensate for surface charging effects, all XPS spectra are referred to the C 1s neutral carbon peak at 284.6 eV. UV-vis absorption spectra were recorded with a U-2000 spectrophotometer. HRESI-TOF-MS spectra were collected on an AB Sciex X500R Q-TOF spectrometer. Elemental analysis (EA) of each relevant species was conducted using a Perkin-Elmer 240 elemental analyzer. Fourier transform infrared (FT-IR) spectra were recorded on a Bruker TENSOR 27 FT-IR spectrometer in the 400-4000 cm⁻¹ region with KBr pellets. EDS measurements were carried out using Zeiss Sigma 500 system. PXRD data were collected at room temperature in air using an X'Pert PRO diffractometer (Cu K α , λ = 1.54178 Å). Luminescence measurements were carried out using a HORIBA FluoroLog-3 fluorescence spectrometer. Steady-state emission spectra were obtained using an East Changing TC202 temperature controller after evacuating each sample for 30 min using a VALUE VRD-16 vacuum pump. Luminescence decays were measured on a HORIBA Scientific Fluorolog-3 spectrofluorometer equipped with a 355-nm laser operating in time-correlated single photon counting mode (TCSPC) with a resolution time of 200 ps. SCXRD measurements were performed on a Rigaku XtaLAB Pro diffractometer with Cu-K α radiation (λ = 1.54184 Å) at 150 K for Cu₁₇ and Ag₁₇. All non-hydrogen atoms were refined with anisotropic thermal parameters, and the hydrogen atoms were included at their idealized positions. Density functional theory (DFT) calculations were performed with Gaussian 09^[S2-S3] using the B3LYP functional.^[S4-S6] Mayer bond-order analysis was conducted by Multiwfn.^[S7]

Synthesis of [Cu₁₇I₃S(C₂B₁₀H₁₀S₂)₆(CH₃CN)₁₁] (Cu₁₇).

Complex Cu₁₇ was synthesized by the reaction of 10 mg 1,2-dithiol-*o*-carborane with 19 mg CuI in 4 mL CH₃CN-THF (v:v = 1:1) at room temperature. The resultant clear solution was allowed to evaporate slowly in darkness at room temperature for three days to give colorless block-like

crystals. Yield: 30% (based on $C_2B_{10}H_{10}S_2H_2$).

Synthesis of $[Ag_{17}I_3S(C_2B_{10}H_{10}S_2)_6(CH_3CN)_{11}] (Ag_{17})$.

Complex Ag_{17} could be synthesized from Cu_{17} by metal-ion exchange: Cu_{17} (0.016 g) were dissolved in 2 mL of CH_2Cl_2 , and 2 mL of 0.1 mM $AgNO_3$ in CH_3CN was added to give a clear reaction solution at room temperature. The resultant solution was allowed to evaporate slowly in darkness at 15 °C for five days to give colorless block-like crystals. Yield: 33% (based on Cu_{17}).

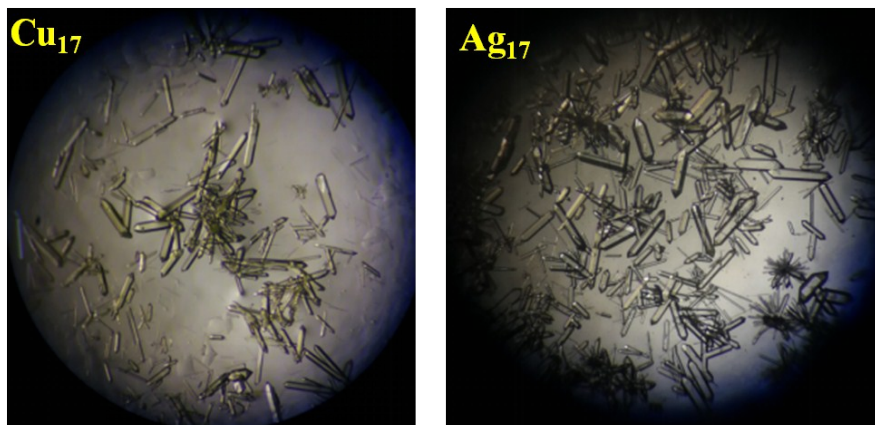


Figure S1. Photographs of as-synthesized Cu_{17} and Ag_{17} crystals, which show similar uniform colorless block morphology. Ten crystals of them were randomly picked out for measurement, which showed virtually identical unit cells (Table S1-2).

Table S1. Unit-cell parameters collected at room temperature of ten Cu_{17} crystals which were randomly picked from one vial shown in Figure S1a.

No.	$a / \text{Å}$	$b / \text{Å}$	$c / \text{Å}$	$\alpha / ^\circ$	$\beta / ^\circ$	$\gamma / ^\circ$	$V / \text{Å}^3$
1	18.873(5)	18.877(6)	24.295(8)	90.08(3)	89.96(3)	119.93(3)	7501(4)
2	18.840(3)	18.845(3)	24.458(5)	90.01(1)	89.94 (2)	120.01(1)	7523(2)
3	18.860(5)	18.873(4)	24.329(5)	90.04 (1)	90.09(2)	119.97(3)	7502(3)
4	18.856(3)	18.857(3)	24.506(4)	89.98(1)	89.98(1)	120.01 (1)	7545(2)
5	18.832(5)	18.844(6)	24.440(5)	89.99(2)	89.99(2)	119.89(3)	7520(3)
6	18.818(6)	18.830(5)	24.342(5)	90.06(1)	89.97(2)	119.88(3)	7479(3)
7	18.876(4)	18.878(3)	24.400(5)	90.05 (1)	90.01(18)	119.98(2)	7531(3)
8	18.874(4)	18.916(5)	24.492(7)	90.09 (2)	90.00(2)	119.97(3)	7575(3)
9	18.853(7)	18.889(7)	24.360(9)	90.06(3)	90.08(3)	119.86(4)	7523(5)
10	18.874(8)	18.889(9)	24.361(7)	90.08(3)	89.98(3)	119.95(5)	7526(5)

Table S2. Unit-cell parameters collected at room temperature of ten **Ag₁₇** crystals which were randomly picked from one vial shown in Figure S1b.

No.	$a / \text{\AA}$	$b / \text{\AA}$	$c / \text{\AA}$	$\alpha / ^\circ$	$\beta / ^\circ$	$\gamma / ^\circ$	$V / \text{\AA}^3$
1	19.606(2)	19.607(2)	24.135(3)	90.04(1)	89.98(9)	120.01(1)	8035(2)
2	19.650(2)	19.651(1)	24.145(4)	90.07(1)	89.95(1)	119.94(1)	8079(2)
3	19.568(9)	19.589(9)	24.166(8)	90.09(3)	90.16(3)	119.95(5)	8029(5)
4	19.600(2)	19.593(3)	24.161(3)	89.99(1)	90.06 (9)	119.98(1)	8038(2)
5	19.619(2)	19.608(2)	24.132(4)	89.98(1)	89.85(1)	120.03(1)	8037(2)
6	19.556(1)	19.550(1)	24.247(19)	90.04(6)	90.03(6)	120.02(8)	8026(1)
7	19.556(7)	19.570(7)	24.178(9)	90.05(3)	89.99(3)	119.93(4)	8019(5)
8	19.571(4)	19.582(4)	24.098(6)	90.17(1)	90.03(1)	120.00(2)	7998(3)
9	19.564(1)	19.581(1)	24.164(11)	90.28(5)	89.88(5)	119.92(8)	8023(8)
10	19.556(1)	19.550(1)	24.247(19)	90.04(6)	90.03(6)	120.02(8)	8026(1)

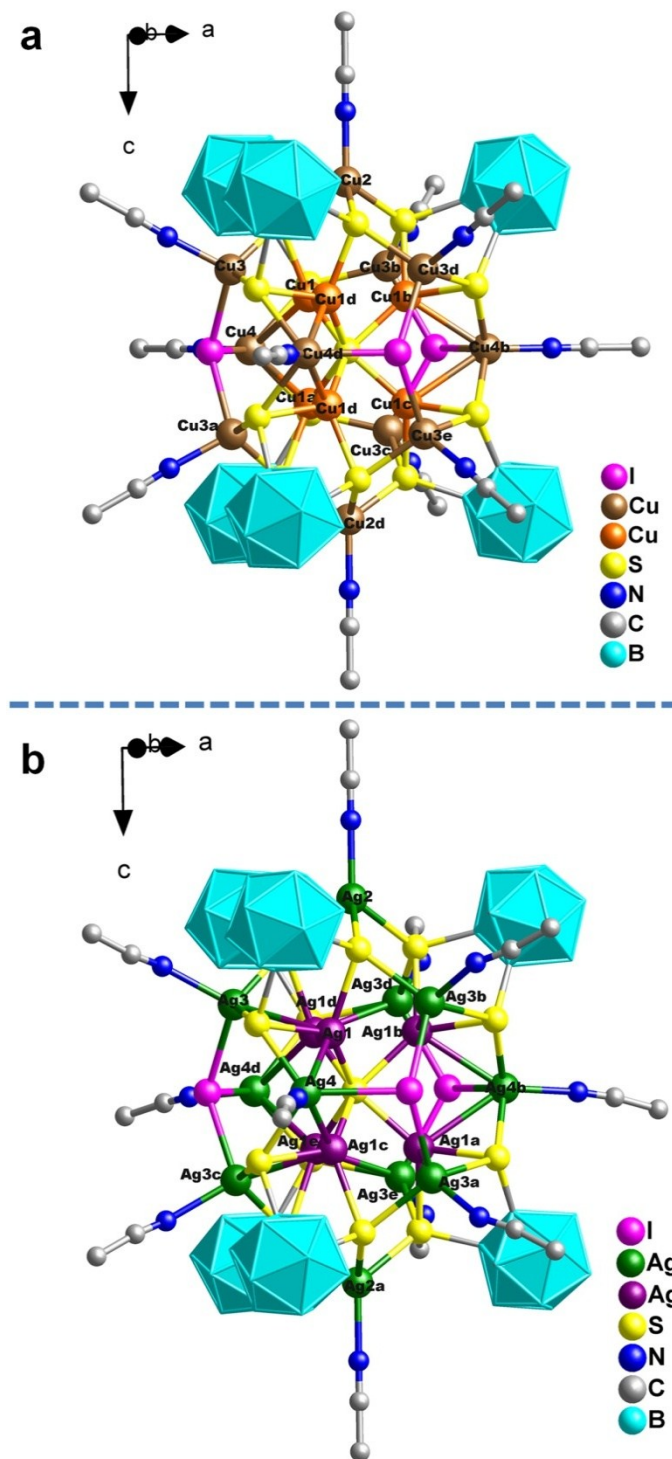


Figure S2. Molecular structures of isomeric **Cu₁₇** and **Ag₁₇** nanoclusters. (a) The structure of $[\text{Cu}_{17}\text{I}_3\text{S}(\text{C}_2\text{B}_{10}\text{H}_{10}\text{S}_2)_6(\text{CH}_3\text{CN})_{11}]$ (**Cu₁₇**) (Cu1-Cu4 2.795 Å; Cu1-Cu3 3.010 Å; Cu1-Cu1¹ 3.024 Å; Cu1-Cu1² 2.929 Å; Cu1-Cu1⁴ 2.929 Å; Cu1-Cu3² 3.011 Å; Symmetry codes: ^a+x, +y, 3/2-z; ^b1-y, 1+x-y, +z; ^c1-y, 1+x-y, 3/2-z; ^d+y-x, 1-x, +z; ^e+y-x, 1-x, 3/2-z). (b) The structure of $[\text{Ag}_{17}\text{I}_3\text{S}(\text{C}_2\text{B}_{10}\text{H}_{10}\text{S}_2)_6(\text{CH}_3\text{CN})_{11}]$ (**Ag₁₇**) (Ag1-Ag4 2.998 Å; Ag1-Ag3 3.092 Å; Ag1-Ag1² 3.144 Å; Ag1-Ag1⁴ 3.144 Å; Ag1-Ag1³ 3.293 Å; Ag1-Ag3² 3.111 Å; Symmetry codes: ^a+y-x, 1-x, 3/2-z; ^b+y-x, 1-x, +z; ^c+x, +y, 3/2-z; ^d1-y, 1+x-y, +z; ^e1-y, 1+x-y, 3/2-z). All H atoms are omitted.

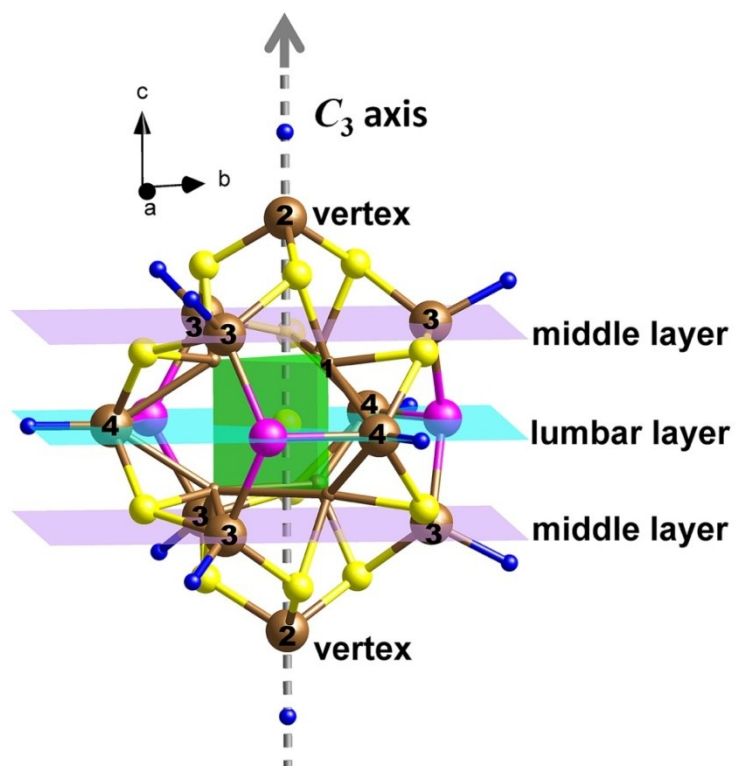


Figure S3. Structure of the Cu_{17} outer shell comprising condensation of nine $(\text{CuI}(\text{NS}_2))$ tetrahedra. The outer shell is considered to have three layers, and the lumbar layer is composed of Cu_3I_3 ; the both layers above and below the lumbar layer consist of three Cu atoms (Cu_3). The number represent Cu2, Cu3 and Cu4 atoms, respectively.

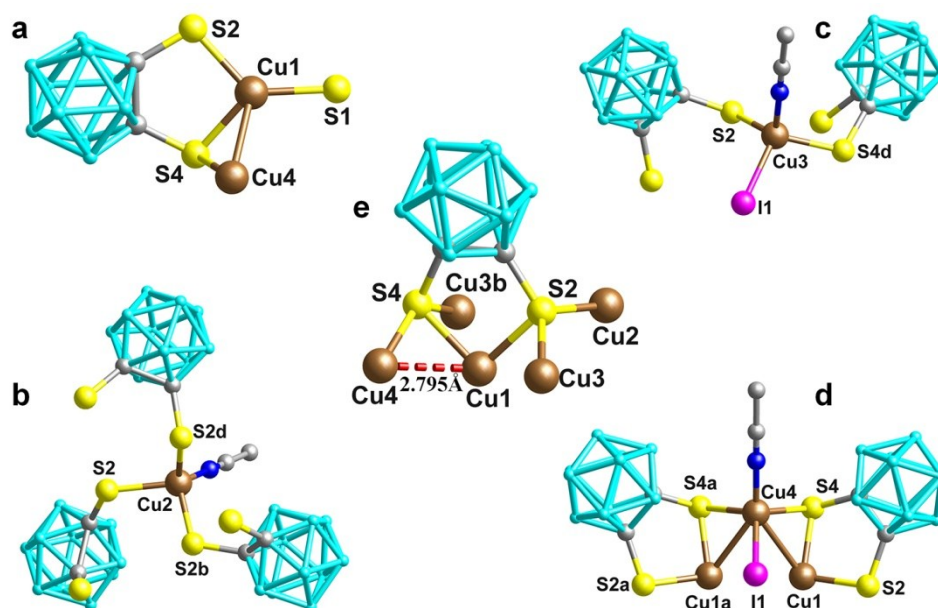


Figure S4. Coordination modes of Cu atoms and thiolate ligands ($C_2B_{10}H_{10}S_2$) in Cu_{17} . The dashed lines represent the Cu...Cu interactions. Color legend: Cu, brown; S, yellow; B, blue; C, gray. Symmetry codes: ^a+x, +y, 3/2-z; ^b1-y, 1+x-y, +z; ^c1-y, 1+x-y, 3/2-z; ^d+y-x, 1-x, +z; ^e+y-x, 1-x, 3/2-z). Direct detection of S^{2-} formed from C-S cleavage of thiolate ligand is very difficult because of the low concentration, as sulfides would be generated with high concentration of S^{2-} . Hence we examined the reaction solution containing 1,2-dithiol-*o*-carborane ($C_2B_{10}H_{10}S_2H_2$) and copper iodide (CuI) in CH_3CN/THF with negative-mode ESI-MS. Fortunately, besides 1,2-dithiol-*o*-carborane in the reaction solution (Figure S5a), the isotopic peaks of a missing S atom species ($C_2B_{10}H_{10}SH^-$) was observed in the mass spectrum, indicating the S-C bond cleavage of the thiol ligands and the possible formation of sulfido groups which are consequently incorporated in the metal clusters (Figure 5b).

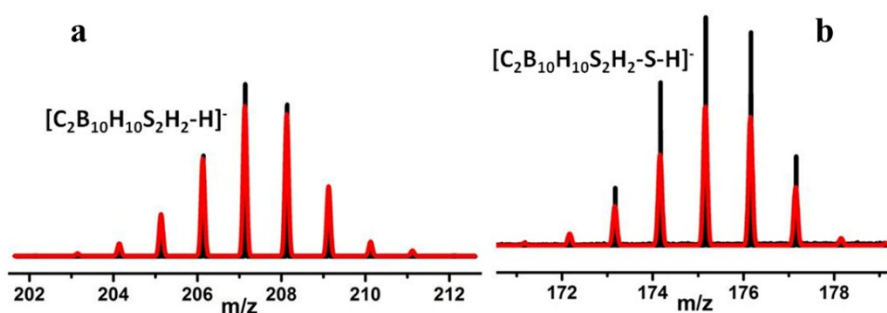


Figure S5. Negative-mode ESI-MS fragment of synthetic reaction solution of Cu_{17} . (a) 1,2-dithiol-*o*-carborane; (b) a S atom missing $C_2B_{10}H_{10}SH^-$ species.

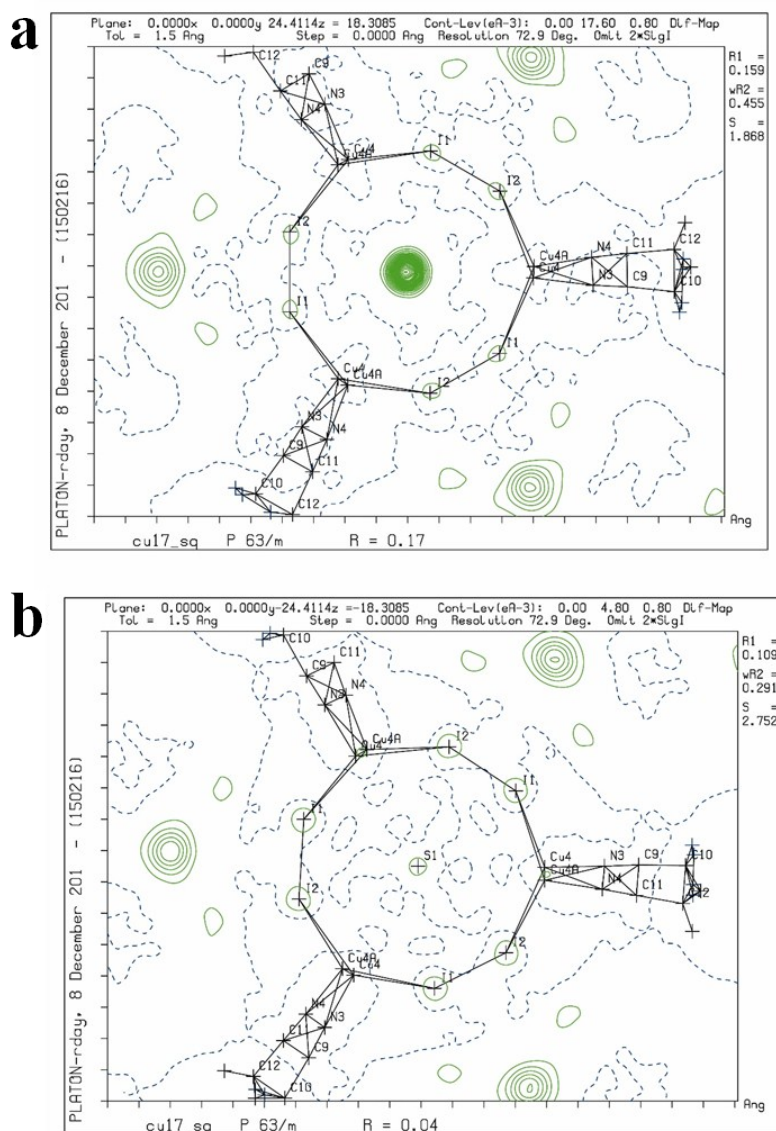


Figure S6. Difference electron density maps of the assigned (a) and unassigned (b) central S atom of the Cu₁₇ cluster generated by PLATON. The blue dotted lines are the zero contours, the green solid lines are positive contours at 0.8 eÅ⁻³ level. According to the single-crystal X-ray structure analysis and charge balance, the high Q peak in the center of the structure was rationally assigned to a S atom rather than metal (Cu, Ag) or non-metal I, C, O and B atom for lower R factors. The difference electron-density maps of the assigned and unassigned central atom of Cu₁₇ generated by PLATON are shown in Figure S6. For the unassigned map, the significant residual electron density is observed in the structure center. After inclusion of the S1 atom, the residual electron density around the S1 site is only about 0.8 eÅ⁻³, indicating that the electron density at this position matches well with that of the assigned S atom.

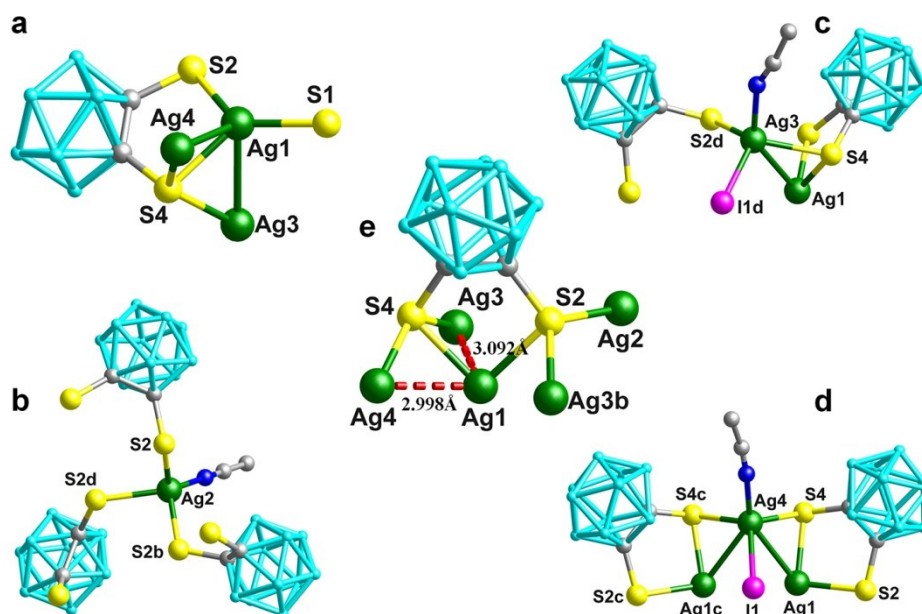


Figure S7. Coordination modes of Ag atom and thiolate ligand ($C_2B_{10}H_{10}S_2$) in Ag_{17} . The dashed lines represent the Ag...Ag interactions. Color legend: Ag, green; S, yellow; B, blue; C, gray. Symmetry codes: $^a+y-x, 1-x, 3/2-z$; $^b+y-x, 1-x, +z$; $^c+x, +y, 3/2-z$; $^d1-y, 1+x-y, +z$; $^e1-y, 1+x-y, 3/2-z$).

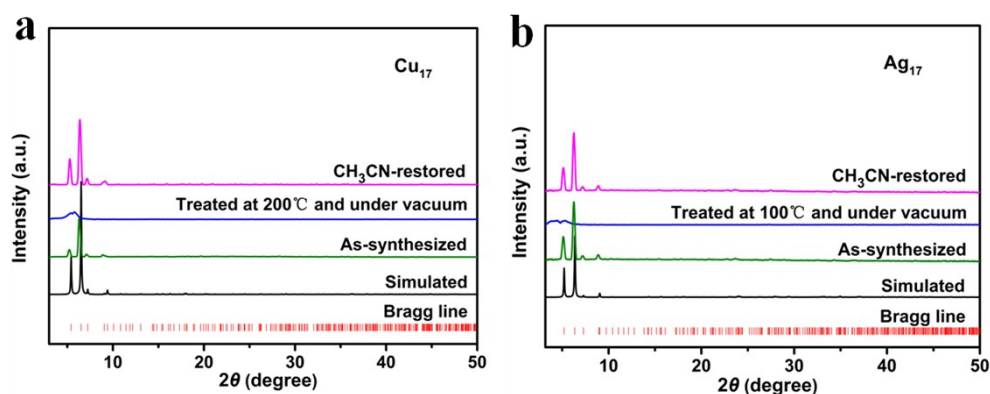


Figure S8. X-ray powder diffraction (PXRD) patterns of Cu_{17} and Ag_{17} . (a) The simulated PXRD pattern from single-crystal data of Cu_{17} overlaps that of the as-prepared crystals, indicating phase purity. Some peaks were not present in the patterns of air-dried Cu_{17} samples, but these peaks were immediately restored after treatment with CH_3CN , indicating that the framework of Cu_{17} remained intact during air drying. (b) An analysis similar to that used for Cu_{17} was applied to Ag_{17} .

As shown in Figure S9, 10.32% weight loss until 330 °C for **Cu₁₇** and 6.56% weight loss until 305 °C for **Ag₁₇** indicate approximately eight and six CH₃CN molecules retained in air-dried **Cu₁₇** and **Ag₁₇** samples, respectively. These findings are consistent with the results of elemental analysis (EA).

For air-dried **Cu₁₇**, [Cu₁₇/I₃S(C₂B₁₀H₁₀S₂)₆(CH₃CN)₈], EA: Cal. H, 2.76; C, 10.94; N, 3.66; S, 13.62. Found H, 2.78; C, 10.90; N, 3.62; S, 13.40.

Theoretical content of eight CH₃CN in air-dried **Cu₁₇**:

$$M_{(\text{CH}_3\text{CN})_8} / M_{[\text{Cu}_{17}/\text{I}_3\text{S}(\text{C}_2\text{B}_{10}\text{H}_{10}\text{S}_2)_6(\text{CH}_3\text{CN})_8]} \times 100\% = 10.73\%$$

Experimental: The percentage of loss mass before 330 °C is found to be 10.32%, which was assigned to the departure of eight CH₃CN molecules.

For air-dried **Ag₁₇**, [Ag₁₇/I₃S(C₂B₁₀H₁₀S₂)₆(CH₃CN)₆], EA: Cal. H, 2.10; C, 7.72; N, 2.25; S, 11.17. Found H, 2.04; C, 8.03; N, 2.54; S, 11.09.

Theoretical content of six CH₃CN in air-dried **Ag₁₇**:

$$M_{(\text{CH}_3\text{CN})_6} / M_{[\text{Ag}_{17}/\text{I}_3\text{S}(\text{C}_2\text{B}_{10}\text{H}_{10}\text{S}_2)_6(\text{CH}_3\text{CN})_6]} \times 100\% = 6.53\%$$

Experimental: The percentage of loss mass before 305 °C is found to be 6.56%, which was assigned to the departure of six CH₃CN molecules.

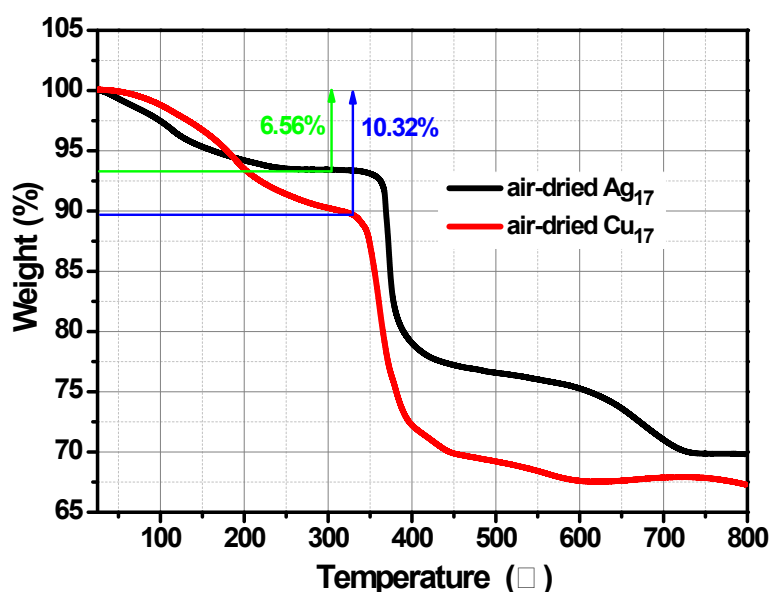


Figure S9. TG plots of air-dried **Cu₁₇** and **Ag₁₇** crystalline samples.

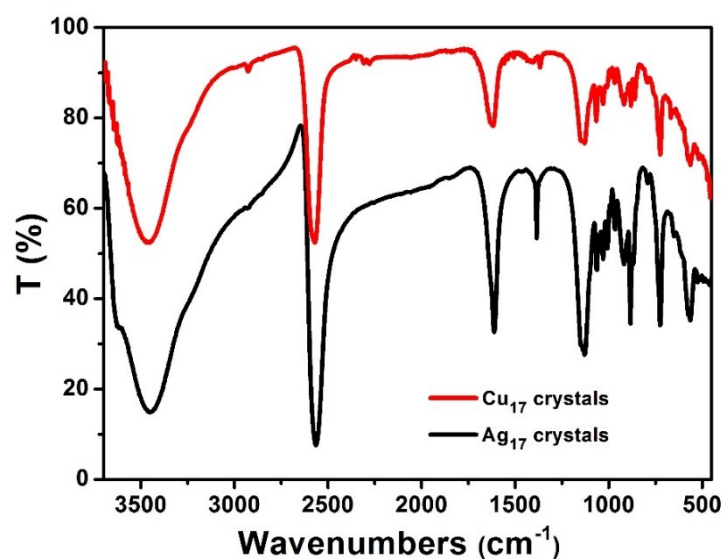


Figure S10. FT-IR spectra of **Cu₁₇** and **Ag₁₇** crystalline samples.

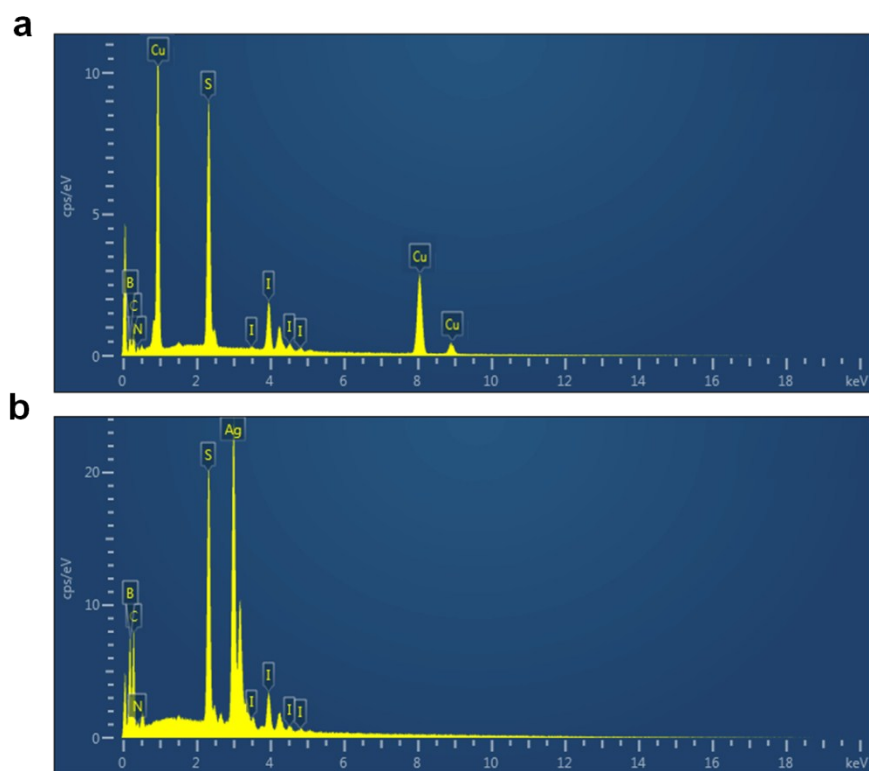


Figure S11. EDS mapping of air-dried **Cu₁₇** and **Ag₁₇** crystals. (a) Cu, I, S, B, C and N are found in the parent **Cu₁₇** cluster. The calculated atomic ratio of Cu : S = 17:13.2 and Cu : I = 17 : 3.0 , which agrees with the formula by SCXRD structural analysis. (b) No traces of Cu were found in the daughter **Ag₁₇** cluster, indicating the total conversion from **Cu₁₇** to **Ag₁₇**, and the expected Ag, I, S, B, C and N are observed. The calculated atomic ratio of Ag : S = 17 : 13.1 and Ag : I = 17 : 3.0, which is in accordance with the formula by SCXRD structural analysis. The amount N element is less because partial coordinated CH₃CN molecules departed, as has been confirmed by TG and elemental analysis results.

As shown in Figure S12 a and b, X-ray photoelectron spectroscopy (XPS) survey spectra showed all the expected elements in **Cu₁₇** and **Ag₁₇**, and no obvious Cu elements observed in **Ag₁₇**, suggesting complete metal exchange from **Cu₁₇** and **Ag₁₇**, which is consistent with the results of SCXRD analysis and EDS analysis. The expanded scans of the specific regions of metal atoms, S and I are shown in Figure S10 c and d. Upon peak fitting, the peak of S 2p_{3/2} at 163.1 eV in **Cu₁₇** and 163.0 eV in **Ag₁₇** can be attributed to thiolate S 2p that is lower than the BE of S in pure solid ligand (1,2-dithiol-*o*-carborane); the peak at 162.4 eV in **Cu₁₇** and 162.0 eV in **Ag₁₇** are assigned to central S²⁻ ions, that corresponds to BE of in Ag₂S nanoparticles.^[58] The atom ratio of thiolate S and center S is calculated to be 12:1 in the two clusters, giving excellent fitting results. The I3d of the two clusters are quite similar and exhibits peaks at 619.9 eV in **Cu₁₇** and 620.0 eV in **Ag₁₇**, respectively. Therefore, an atomic ratio of 12:1 for thiolate S and S ions from XPS analysis also further support this formula **Cu₁₇** and **Ag₁₇**.

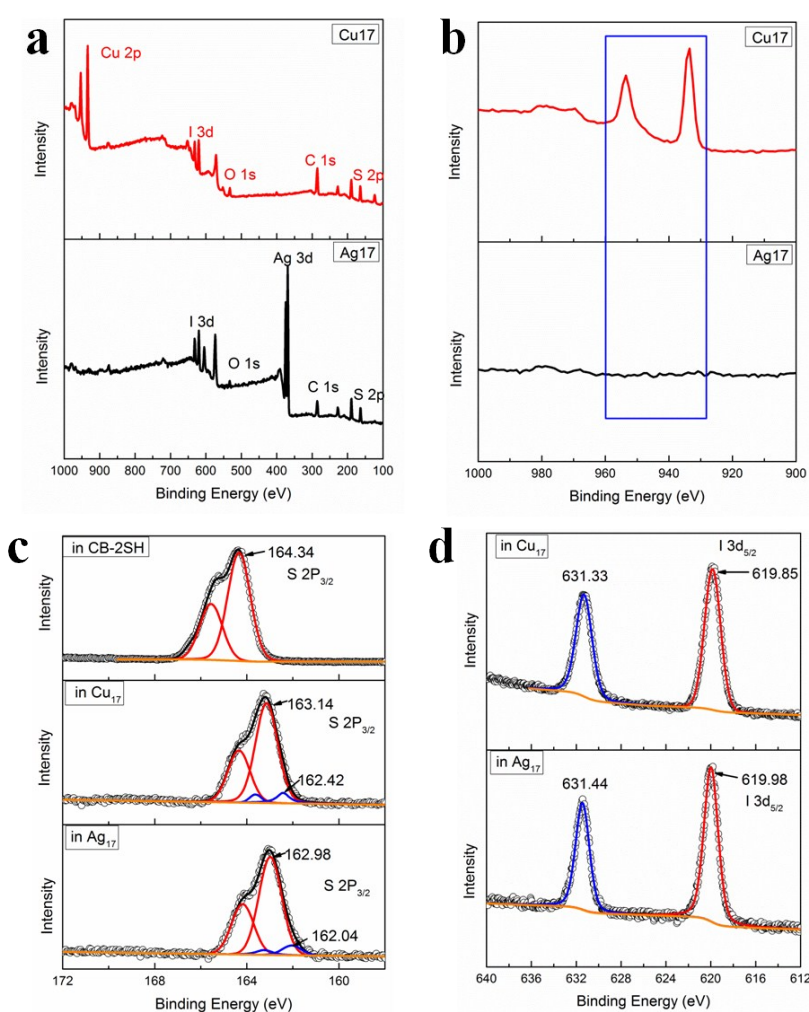


Figure S12. (a, b) XPS survey spectrum of **Cu₁₇** and **Ag₁₇** cluster and the enlargement of the region between 900-1000 eV, suggesting no obvious Cu in **Ag₁₇** crystals and complete metal exchange from **Cu₁₇** to **Ag₁₇**. (c, d) The high-resolution XPS of S 2p and I 3d, respectively.

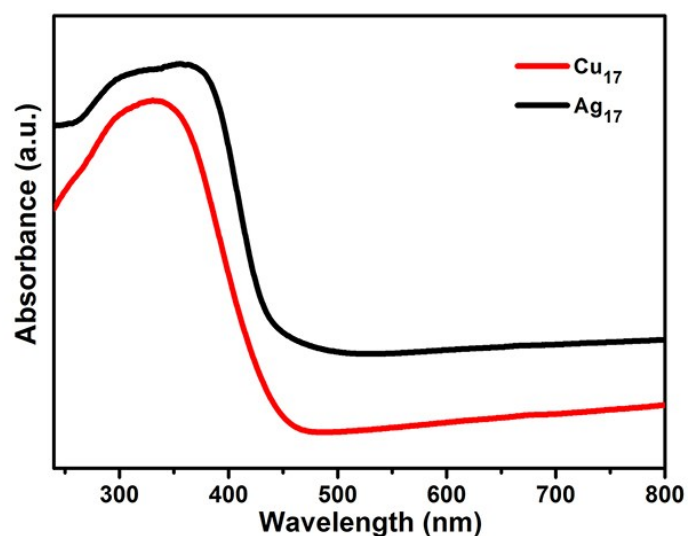


Figure S13. UV-vis diffuse reflectance spectra of **Cu₁₇** and **Ag₁₇** solid-state samples containing a small quantity of **CH₃CN**.

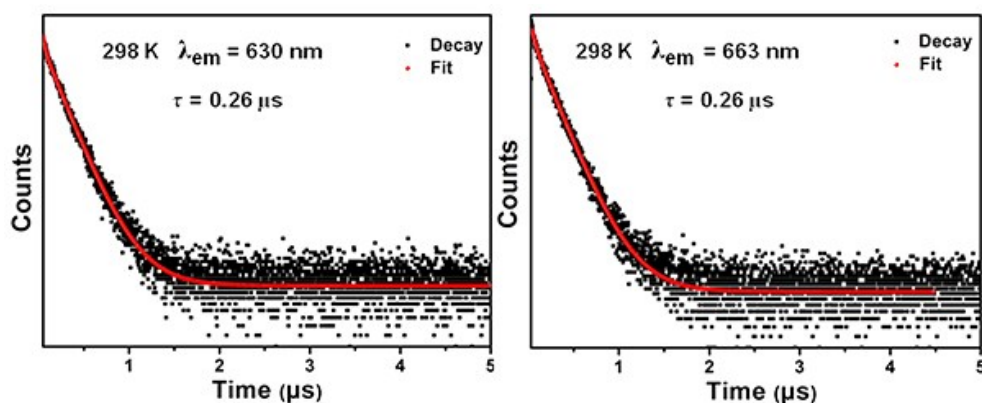


Figure S14. PL decays of a fluid solution of **Cu₁₇** in **CH₂Cl₂/CH₃CN** at 298 K. The identical lifetimes of the emissive peaks at 630 nm and 663 nm suggest that the emission probably originates from the same excited state (excited at 355 nm).

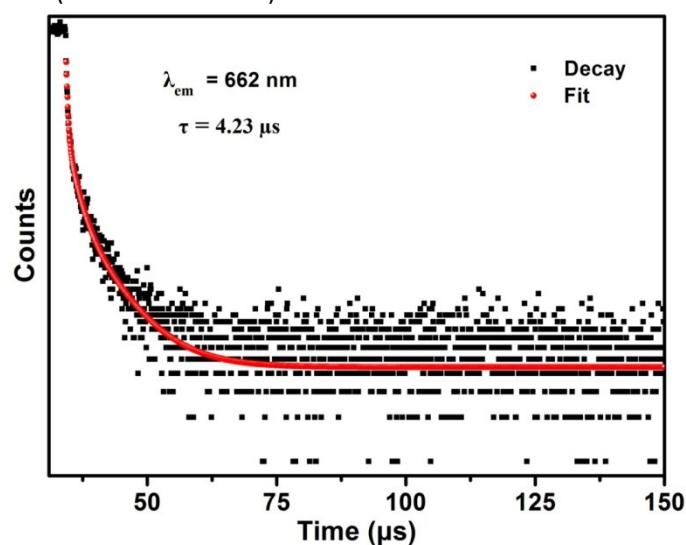


Figure S15. PL decay of a fluid solution of **Ag₁₇** in **DMF/CH₃CN** at 240 K. The microsecond-long lifetime of the peak at 662 nm demonstrates the inherent phosphorescence of the system

(excited at 355 nm).

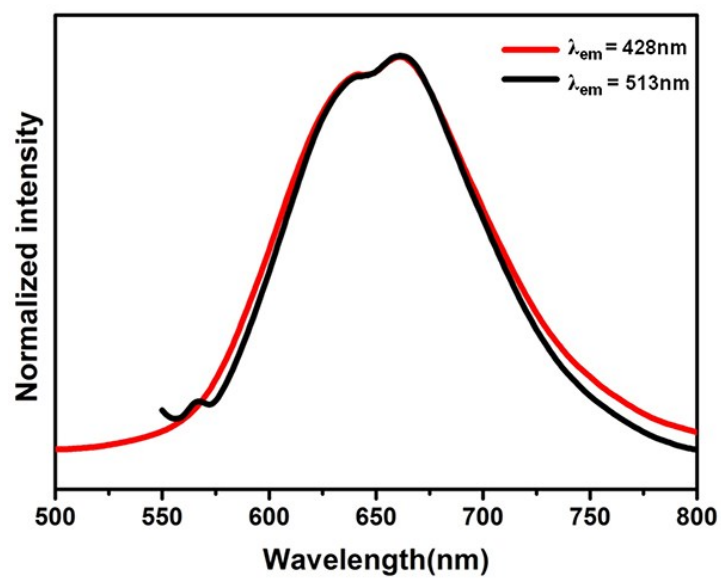


Figure S16. Excitation-dependent emission spectra of Ag_{17} in liquid $\text{DMF}/\text{CH}_3\text{CN}$ (240 K). The intensities have been normalized.

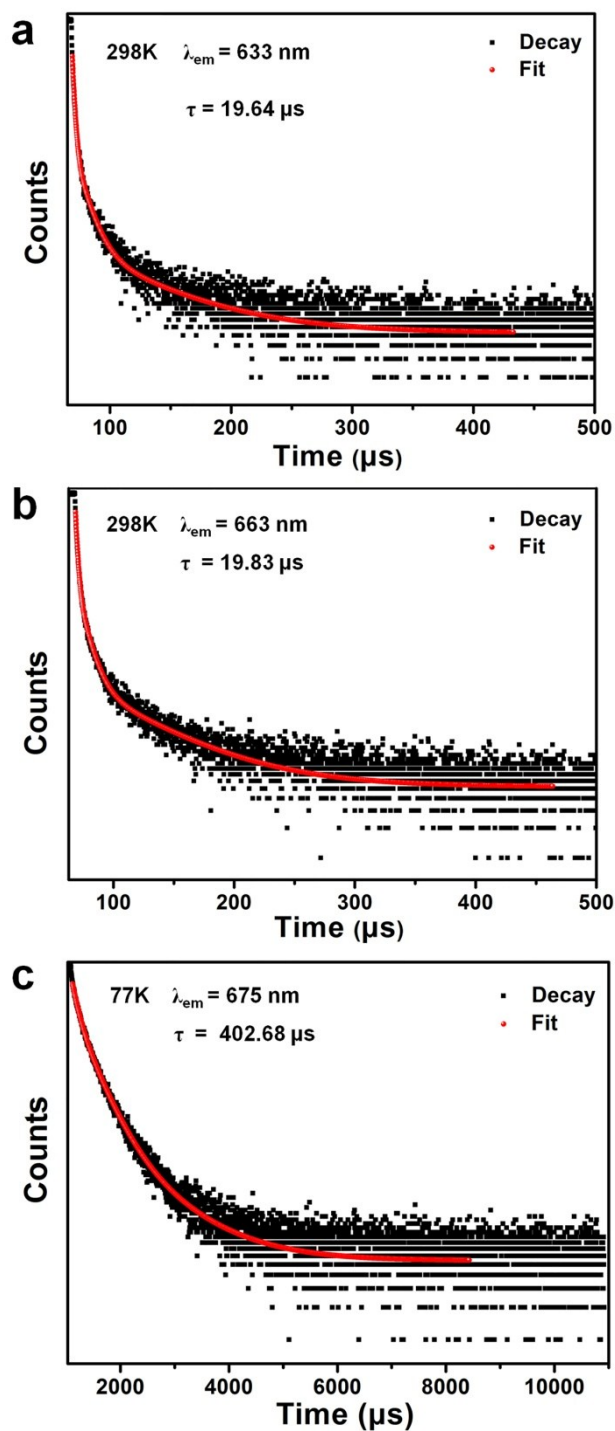


Figure S17. PL decays of Cu_{17} in the solid state and in a frozen matrix. (a, b) PL decays at 633 nm and 663 nm of Cu_{17} in the solid state at 298 K. (c) PL decays of Cu_{17} frozen in $\text{CH}_2\text{Cl}_2/\text{CH}_3\text{CN}$ at 77 K (excited at 355 nm).

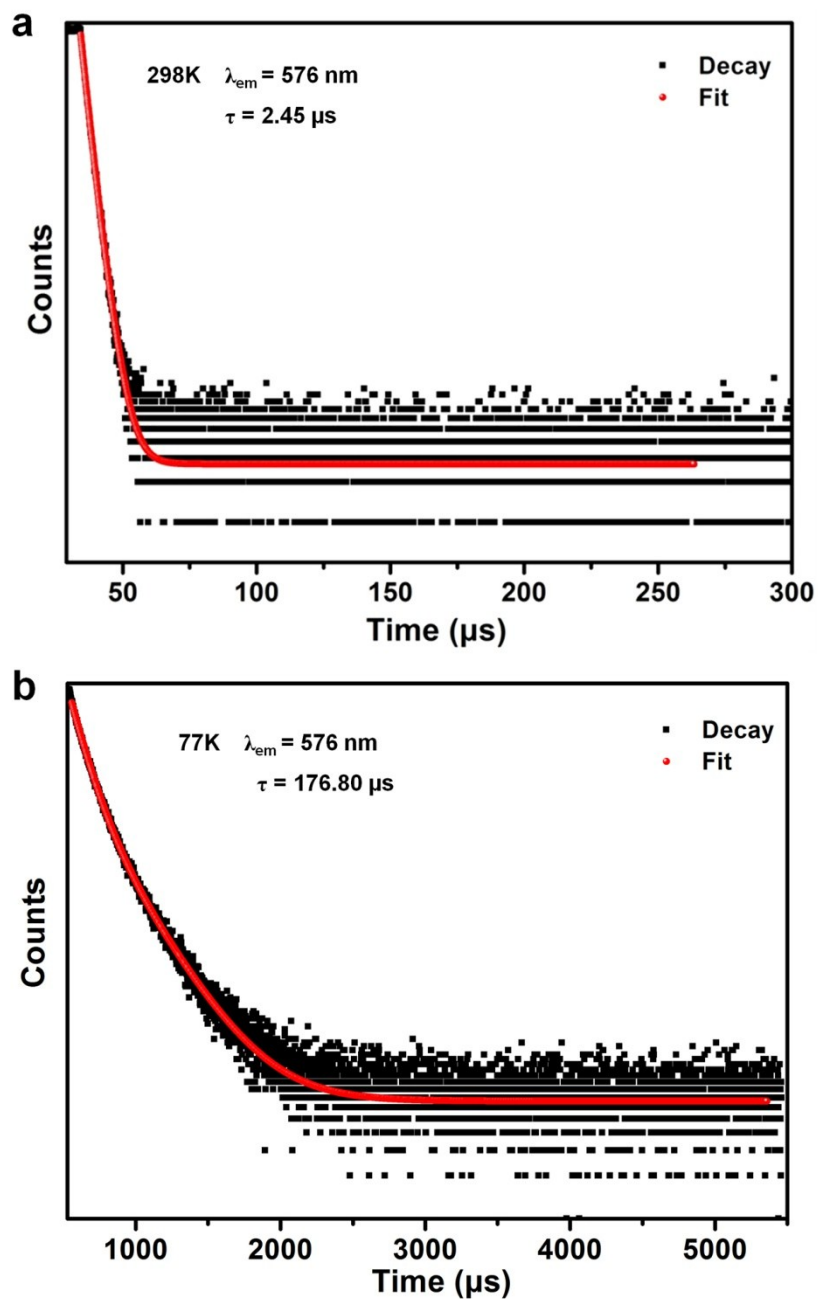


Figure S18. PL decays of Ag_{17} in the solid state and in a frozen matrix. (a) PL decays at 576 nm of solid-state Ag_{17} samples with a small quantity of CH_3CN . (b) PL decays at 576 nm of Ag_{17} in a frozen DMF/ CH_3CN at 77 K.

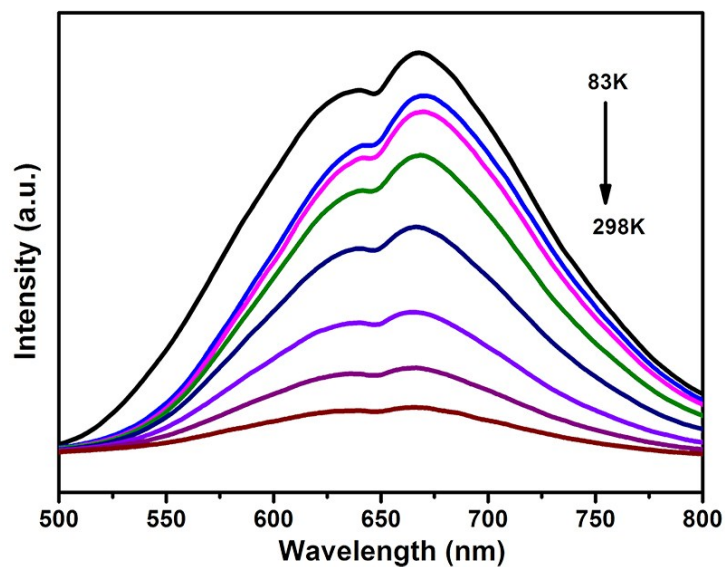


Figure S19. Temperature-dependent emission spectra of partially CH_3CN -lost Cu_{17} in the solid state. Solid-state Cu_{17} samples were obtained by air drying, and approximately three CH_3CN molecules escaped from the coordination shell of the Cu_{17} clusters. The PL measurements were performed in ambient environment.

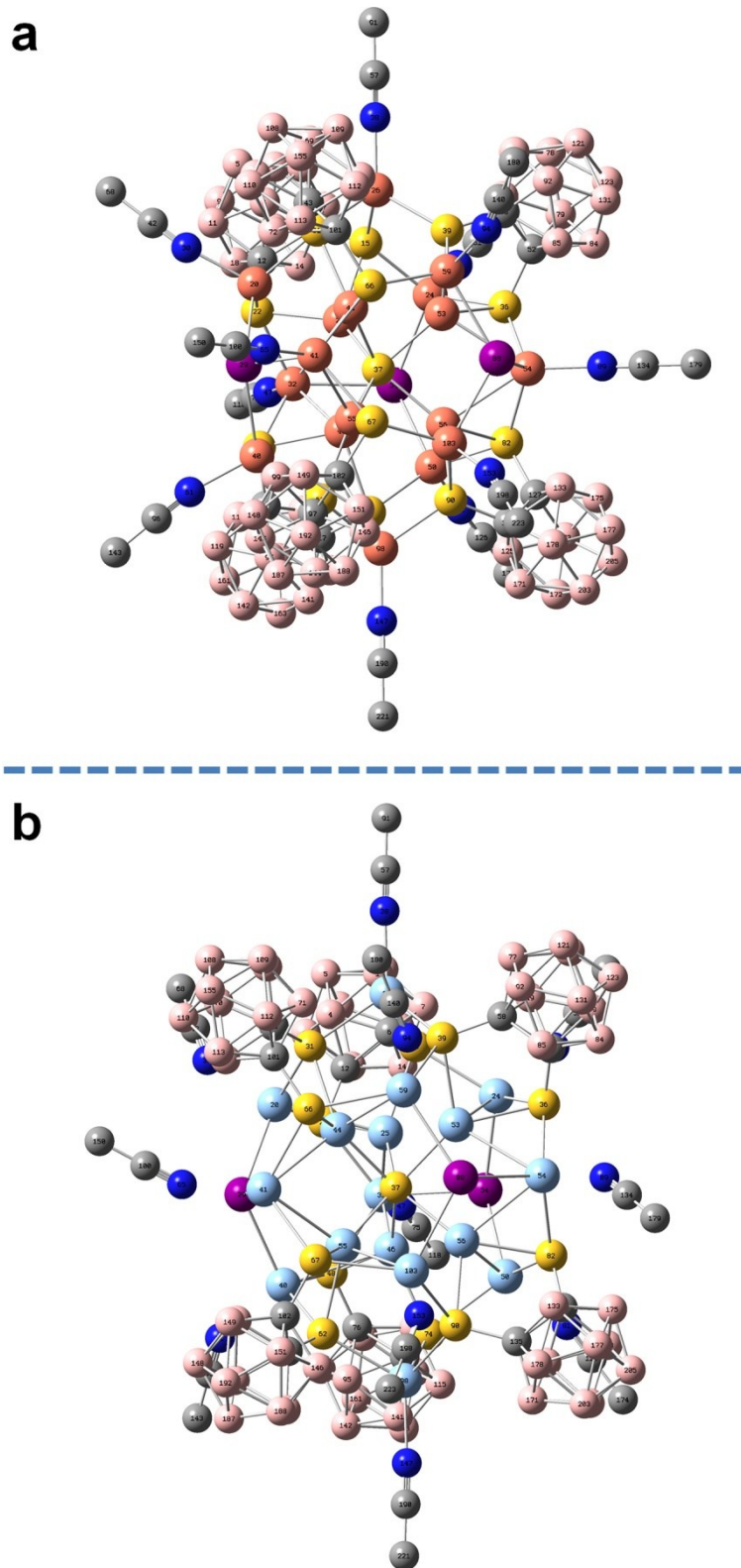


Figure S20. Optimized structures of the **Cu₁₇** and **Ag₁₇** clusters. (a) The six shortest Cu...Cu distances in **Cu₁₇** are 2.77 Å. (b) There are six Ag...Ag distances of 3.05-3.06 Å and six of 3.20-3.21 Å in **Ag₁₇**. All H atoms are omitted.

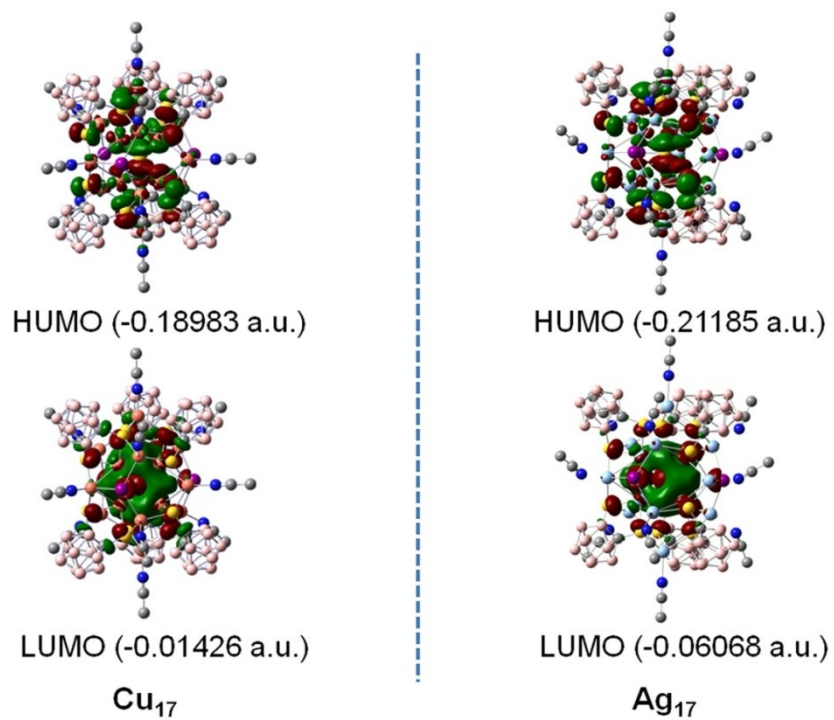


Figure S21. MOs of the **Cu₁₇** and **Ag₁₇** clusters. The numbers in parentheses denote the energies of the HOMO and LUMO levels.

Table S3. Crystal data and structure refinement parameters of **Cu₁₇** and **Ag₁₇**.

	Cu₁₇	Ag₁₇
CCDC number	1868508	1868509
Empirical formula	C ₃₄ H ₉₃ B ₆₀ Cu ₁₇ I ₃ N ₁₁ O ₅ S ₁₃	C ₃₄ H ₉₃ B ₆₀ Ag ₁₇ I ₃ N ₁₁ S ₁₃
Formula weight	3262.38	3935.98
Temperature/K	150.00(10)	150.00(10)
Crystal system	hexagonal	hexagonal
Space group	<i>P6₃/m</i>	<i>P6₃/m</i>
<i>a</i> /Å	18.8251(4)	19.5485(4)
<i>b</i> /Å	18.8251(4)	19.5485(4)
<i>c</i> /Å	24.4114(5)	24.1925(8)
α /°	90	90
β /°	90	90
γ /°	120	120
Volume /Å ³	7492.0(4)	8006.4(4)
Z	2.00004	2.00004
ρ_{calc} g/cm ³	1.446	1.633
μ /mm ⁻¹	9.309	22.572
F(000)	3148.0	6438.0
Crystal size/mm ³	0.3 × 0.21 × 0.2	0.3 × 0.2 × 0.1
Radiation	Cu K α (λ = 1.54184)	Cu K α (λ = 1.54184)
2 θ range for data collection /°	6.52 to 145.824	6.372 to 146.438
Index ranges	-23 ≤ <i>h</i> ≤ 22, -22 ≤ <i>k</i> ≤ 22, -20 ≤ <i>l</i> ≤ 29	-24 ≤ <i>h</i> ≤ 11, -14 ≤ <i>k</i> ≤ 17, -29 ≤ <i>l</i> ≤ 25
Reflections collected	29293	26402
Independent reflections	5052 [<i>R</i> _{int} = 0.0482, <i>R</i> _{sigma} = 0.0377]	5415 [<i>R</i> _{int} = 0.0903, <i>R</i> _{sigma} = 0.0570]
Data/restraints/parameters	5052/74/377	5415/120/254
Goodness-of-fit on F ²	1.026	1.132
Final R indexes [<i>I</i> >= 2 σ (<i>I</i>)]	<i>R</i> ₁ = 0.0765, <i>wR</i> ₂ = 0.2301	<i>R</i> ₁ = 0.0928, <i>wR</i> ₂ = 0.2527
Final R indexes [all data]	<i>R</i> ₁ = 0.0942, <i>wR</i> ₂ = 0.2601	<i>R</i> ₁ = 0.0995, <i>wR</i> ₂ = 0.2629
Largest diff. peak/hole / e Å ⁻³	2.25/-3.01	3.21/-2.53

$$R_1 = \sum ||F_o| - |F_c|| / \sum |F_o|. \quad wR_2 = [\sum w(F_o^2 - F_c^2)^2 / \sum w(F_o^2)^2]^{1/2}$$

Table S4. Select bond lengths [Å] in **Cu₁₇** and **Ag₁₇**.

Cu₁₇			
Cu1-Cu4	2.7950(7)	Cu3-S2	2.3480(2)
Cu1-S1	2.2682(5)	Cu3-S4 ⁴	2.3160(2)
Cu1-S2	2.3030(2)	Cu4-S4	2.5440(6)
Cu1-S4	2.3000(2)	Cu3-I1	2.6761(7)
Cu2-S2	2.3410(2)	Cu4-I1	2.6110(7)
Symmetry codes: ¹ +x, +y, 3/2-z; ² 1-y, 1+x-y, +z; ³ 1-y, 1+x-y, 3/2-z; ⁴ +y-x, 1-x, +z			
Ag₁₇			
Ag1-Ag4	2.9980(2)	Ag3-S2 ⁴	2.5650(5)
Ag1-Ag3	3.0920(2)	Ag3-S4	2.6610(5)
Ag1-S1	2.4504(12)	Ag4-S4	2.5940(5)
Ag1-S2	2.5380(6)	Ag3 ¹ -I1	2.8426(17)
Ag1-S4	2.4940(5)	Ag4-I1	2.9400(3)
Ag1-S2	2.5830(5)		
Symmetry codes: ¹ +y-x, 1-x, 3/2-z; ² +y-x, 1-x, +z; ³ +x, +y, 3/2-z; ⁴ 1-y, 1+x-y, +z			

Table S5. Calculated Cu-Cu bond orders in Cu₁₇ and Ag-Ag bond orders in Ag₁₇.

Cu-Cu bond order of Cu ₁₇					
20(Cu)	26(Cu)	0.07683811	41(Cu)	55(Cu)	0.12796015
20(Cu)	41(Cu)	0.05198729	44(Cu)	53(Cu)	0.10955584
24(Cu)	26(Cu)	0.07675559	44(Cu)	55(Cu)	0.10852111
24(Cu)	32(Cu)	0.05223513	46(Cu)	55(Cu)	0.10942942
25(Cu)	32(Cu)	0.12816930	46(Cu)	56(Cu)	0.10923140
25(Cu)	44(Cu)	0.10975193	50(Cu)	98(Cu)	0.07663225
25(Cu)	46(Cu)	0.10776284	53(Cu)	54(Cu)	0.12837670
25(Cu)	53(Cu)	0.10996172	53(Cu)	56(Cu)	0.10755166
26(Cu)	59(Cu)	0.07659084	54(Cu)	56(Cu)	0.12736311
32(Cu)	46(Cu)	0.12735466	54(Cu)	59(Cu)	0.05211944
32(Cu)	50(Cu)	0.05189868	54(Cu)	103(Cu)	0.05175470
40(Cu)	41(Cu)	0.05183621	55(Cu)	56(Cu)	0.10939726
40(Cu)	98(Cu)	0.07664557	98(Cu)	103(Cu)	0.07658039
41(Cu)	44(Cu)	0.12780661			
Ag-Ag bond order of Ag ₁₇					
20(Ag)	26(Ag)	0.13763399	41(Ag)	44(Ag)	0.10490550
20(Ag)	32(Ag)	0.07322264	41(Ag)	55(Ag)	0.10518764
20(Ag)	40(Ag)	0.06519477	41(Ag)	59(Ag)	0.07276715
20(Ag)	41(Ag)	0.09760847	41(Ag)	103(Ag)	0.07288089
24(Ag)	26(Ag)	0.13726455	44(Ag)	53(Ag)	0.21127898
24(Ag)	32(Ag)	0.09854265	44(Ag)	55(Ag)	0.10954847
24(Ag)	50(Ag)	0.06530382	46(Ag)	55(Ag)	0.21121121
24(Ag)	54(Ag)	0.07338386	46(Ag)	56(Ag)	0.21134067
25(Ag)	32(Ag)	0.10656642	50(Ag)	54(Ag)	0.07277818
25(Ag)	44(Ag)	0.21144857	50(Ag)	98(Ag)	0.13712268
25(Ag)	46(Ag)	0.10804474	53(Ag)	54(Ag)	0.10676271
25(Ag)	53(Ag)	0.21223084	53(Ag)	56(Ag)	0.10753767
26(Ag)	59(Ag)	0.13688695	54(Ag)	56(Ag)	0.10427913
26(Ag)	98(Ag)	0.09467248	54(Ag)	59(Ag)	0.09818302
32(Ag)	40(Ag)	0.07252156	54(Ag)	103(Ag)	0.09704607
32(Ag)	46(Ag)	0.10420065	55(Ag)	56(Ag)	0.21143888
32(Ag)	50(Ag)	0.09739495	59(Ag)	103(Ag)	0.06533683
40(Ag)	41(Ag)	0.09715228	98(Ag)	103(Ag)	0.13720223
40(Ag)	98(Ag)	0.13726666			

References

- [S1] C. Viñas, R. Benakki, F. Teixidor and J. Casabó, *J. Inorg. Chem.*, 1995, **34**, 3844–3845.
- [S2] M. J. Frisch, et al. Gaussian, Inc., Wallingford CT, 2009.
- [S3] A. D. Becke, *J. Chem. Phys.*, 1993, **98**, 5648–5652.
- [S4] C. Lee, W. Yang and R. G. Parr, *Phys. Rev. B* 1988, **37**, 785–789.
- [S5] S. H. Vosko, L. Wilk and M. Nusair, *Can. J. Phys.*, 1980, **58**, 1200–1211.
- [S6] P. J. Stephens, F. J. Devlin, C. F. Chabalowski and M. J. Frisch, *J. Phys. Chem.*, 1994, **98**, 11623–11627.
- [S7] T. Lu and F. W. Chen, *J. Comput. Chem.*, 2012, **33**, 580-592.
- [S8] M. Pang, J. Hu and H. C. Zeng, *J. Am. Chem. Soc.*, 2010, **132**, 10771-10785.